

Review

Research Progress of Anode-Free Lithium Metal Batteries

Jian Zhang ^{1,†} , Abrar Khan ^{1,†}, Xiaoyuan Liu ¹, Yuban Lei ², Shurong Du ¹, Le Lv ³, Hailei Zhao ^{4,*} 
and Dawei Luo ^{1,*} ¹ School of Materials and Environmental Engineering, Shenzhen Polytechnic, Shenzhen 518055, China² College of Intelligent Metallurgy, Guangxi Modern Polytechnic College, Hechi 547000, China³ School of Applied Biology, Shenzhen Institute of Technology, Shenzhen 518116, China⁴ School of Materials Science and Engineering, University of Science and Technology Beijing, Beijing 100083, China

* Correspondence: hlzhao@ustb.edu.cn (H.Z.); luodw@szpt.edu.cn (D.L.)

† These authors contributed equally to this work.

Abstract: Lithium-metal batteries (LMBs) are regarded as the most promising candidate for practical applications in portable electronic devices and electric vehicles because of their high capacity and energy density. However, the uncontrollable growth of lithium dendrite reduces its cycling ability and even causes a severe safety concern, which impedes the development of the technology. Although great efforts have been devoted to solving the lithium dendrite issue in recent years, the contradiction between the high cost of thin Li foil and the severe safety hazard of excess Li still exists. This is precisely the factor that inspired the development of anode-free lithium-metal batteries (AFLMBs). Compared to lithium-metal batteries, AFLMBs with a zero-excess Li anode possess an incredible, conceivable, and specific energy. Additionally, because the use of metal lithium is limited, the battery manufacturing will be safer and simpler, leading to a significant decrease in cost. However, comprehensive reviews on anode-free batteries are rare. Therefore, in this review, we aim to explain the essential development factors influencing the cycle life, energy density, cost, and working mechanism of anode-free batteries. We summarize different strategies to improve the cycling stability of AFLMBs, and we discuss the application of anode-free electrodes in other electrochemical energy storage systems. Moreover, it is believed that the combination of modification techniques, including electrolytes and current collectors, and the application protocols will be the most important solution for future anode-free batteries.

Keywords: anode-free; lithium-ion batteries; lithium-metal batteries; lithium dendrite



Citation: Zhang, J.; Khan, A.; Liu, X.; Lei, Y.; Du, S.; Lv, L.; Zhao, H.; Luo, D. Research Progress of Anode-Free Lithium Metal Batteries. *Crystals* **2022**, *12*, 1241. <https://doi.org/10.3390/cryst12091241>

Academic Editor: Yutaka Moritomo

Received: 4 August 2022

Accepted: 26 August 2022

Published: 2 September 2022

Publisher's Note: MDPI stays neutral with regard to jurisdictional claims in published maps and institutional affiliations.



Copyright: © 2022 by the authors. Licensee MDPI, Basel, Switzerland. This article is an open access article distributed under the terms and conditions of the Creative Commons Attribution (CC BY) license (<https://creativecommons.org/licenses/by/4.0/>).

1. Introduction

Since lithium-ion batteries (LIBs) first entered the market in 1991, they have completely changed our lives, laying the foundation for a wireless and fossil-fuel-free society, thus representing great benefit to mankind. At present, LIBs have a wide range of applications, e.g., the mainstream energy storage form of portable electronic equipment, new energy vehicles, and smart grids [1]. With continuous development, the application scenario also puts forward higher requirements for the energy density of the battery. However, the energy density of the available commercial LIBs has reached a bottleneck and is less than 250 Wh·kg⁻¹ [2]. Although we have seen great progress made in the laboratory, there is still a long way to go to achieve an energy density of 500 Wh·kg⁻¹ [3,4]. For example, by adjusting the content of nickel in ternary cathode material, the reversible specific capacity of the cathode material will also change. Compared with the current value, it can be increased by up to 40% [5–7]. The mixture of silicon and graphite can also deliver improvements to the specific capacity [8,9]. However, there are still many problems to be solved from laboratory to industrialization for practical applications, and the optimal results cannot meet the goal. Anode-free batteries and lithium-metal batteries provide high volumetric and gravimetric energy density, compared to Li-ion batteries.

At present, the anode material of commercial lithium-ion batteries is mainly graphite, and its actual specific capacity is very close to its theoretical specific capacity. In order to further improve the specific capacity of the battery, a variety of new anode materials, such as Sn, Sb, and Si, have been developed in recent years. These anode materials generally form a battery system with lithium-containing cathode materials. Lithium-containing transition-metal-layered compounds are ideal for cathode materials because of their high voltage and moderate specific capacity. At the same time, lithium has become a popular metal in high-energy-density lithium batteries due to its high theoretical specific capacity and the most negative electrode potential. In the lithium-metal battery, the lithium source can be provided by the negative electrode; hence, the positive electrode should be a compound without lithium and the ability to store lithium. At present, lithium-free cathode materials, such as iron sulfide, graphite fluoride, and manganese dioxide, have a low potential for lithium removal, which is bound to affect energy density improvement. At this time, if we continue to use the original mature transition metal oxide as the cathode material and make use of its high-voltage, lithium-containing, and mature process characteristics, the negative electrode will save active material. It allows the lithium in the positive electrode to be deposited directly onto the negative collector during the charge and discharge process, to build an anode-free electrochemical system. It is expected to become an important development direction of the next generation of high-energy density batteries. Due to the lowest redox potential (-3.04 V vs. SHE), the lithium metal is considered as the ideal anode material with its maximum theoretical capacity of up to $3860 \text{ mAh}\cdot\text{g}^{-1}$, $2061 \text{ mAh}\cdot\text{cm}^{-3}$ for anode materials [10,11]. Therefore, the lithium metal anode is the most significant factor allowing a quantum leap in the lithium-ion energy density of batteries.

Recently, various computational studies have been used to facilitate the rationalization of the Li^+ transport mechanism, the Li deposition behavior, etc. Via simulations and experimental measurements and analyses, the beneficial effect of electron deficiency on the Li hosting behavior of the carbon current collector was demonstrated. They also reported the results of testing anode-free coin cells comprising a multivacancy defective carbon current collector; these cells retained 90% of their initial capacity for over 50 cycles under lean electrolyte conditions [12].

Meanwhile, lithium metal plays an important role in the structure of advanced lithium-sulfur batteries and lithium-oxygen batteries. They all have some common defects, including low coulombic efficiency, poor rate reversibility, thermal runaway, and other safety issues due to lithium dendrites, which can cause depletion, undesirable side reactions, and short-circuits [13–15]. To improve the LMB performance, many researchers have developed state-of-the-art optimization procedures and systematically studied the intrinsic regulation principles for better lithium anode stability, according to the recent literature [16–18]. However, the attained specific capacity is still a problem [11]. In order to improve the coulombic efficiency and enhance the life cycling of batteries, the concept of anode-free batteries was proposed, whereby the material on the surface of the current collector is very thin or there are self-assembled materials without a current collector. Not only does the battery have only a cathode, but it is organized in a different manner compared to Li-ion and Li-metal batteries.

2. Anode-Free Batteries

LIBs are mainly designed in configurations such as $\text{Cu}/\text{C}_6/\text{PP}/\text{LiXO}/\text{Al}$ arrangements, where Al and Cu represent the current collectors, and C_6 is used as the graphite anode. In terms of energy storage capacity, PP denotes the separator from polymer materials, while LiXO represents the lithiated oxide cathode, e.g., LCO, LMO, NCA, and LFP. Lithium metal shows excellent performance with advantages such as being lightweight, providing an excellent specific capacity, and showing a high negative standard potential window compared with other anode materials. Furthermore, lithium-ion batteries using lithium metal as the anode could provide excellent electrochemical performance with a higher potential window than the graphite anode by about 0.1 V, while the en-

ergy density can also be improved [19]. However, the formation of dendrites during the charge–discharge processes decreases the coulombic efficiency. A parasitic reaction with the surrounding electrolytes mostly happens in the batteries during charging and discharging via the organic electrolyte. Anodes with greater Li metal excess have recently been used in many areas. Nevertheless, the attained specific capacity is not satisfactory [11]. Several techniques have been developed to improve the coulombic efficiency and enhance the life cycling of anode-free batteries. Figure 1 summarizes the recent studies, including optimization of the electrolyte and current collector, as well as design of the most favorable protocols.

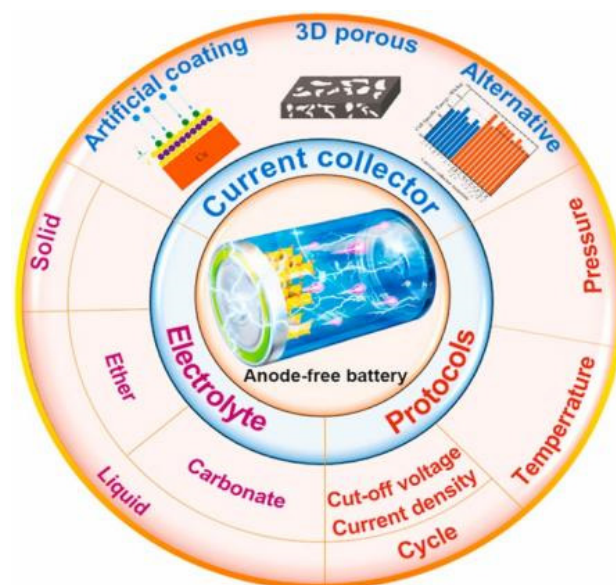


Figure 1. Schematic diagram of anode-free batteries. “Reprinted from The Lancet, Vol. number, Author(s), Title of article, Pages No., Copyright (2006), with permission from Elsevier”.

For instance, by increasing the Li content to over 200%, the theoretical capacity of lithium-metal batteries in terms of volumetric energy density declines from $687 \text{ mAh}\cdot\text{L}^{-1}$ to $2060 \text{ mAh}\cdot\text{L}^{-1}$. The specific capacity of LMB is even lesser than when using graphite as anode, which can provide $719 \text{ mAh}\cdot\text{L}^{-1}$ [20]. Furthermore, if the Li anode’s thickness exceeds $50 \mu\text{m}$, the failure operation at an early stage is reduced by a quick reduction in the lean electrolyte [21,22].

Liu and coworkers reported that, when using a thin electrolyte, the cycle life of the battery with $250 \mu\text{m}$ Li foil decreases sixfold, with even the concentrated electrolyte failing to have an effect. When the Li foil thickness is about $50 \mu\text{m}$, the cycle life is still 20 cycles. Moreover, a massive quantity of Li metal in the batteries can lead to fire and explosions following car accidents or bad weather. In some cases, companies have recalled their products and paid a heavy price for the accidents.

Therefore, decreasing the amount of Li by using a thin Li anode of less than $50 \mu\text{m}$ (the ideal thickness is $20 \mu\text{m}$) could provide a higher energy density with excellent industrial application safety [23]. For example, Zhang and coworkers prepared a Li metal battery containing an excess amount of Li, and the thickness of the foil was $45 \mu\text{m}$. Furthermore, the prepared cathode was evaluated using a prepared electrolyte, which could provide a 12 times higher life cycle [24]. In the meantime, Park’s group manufactured a Li metal battery with Li anode of $20 \mu\text{m}$ thickness. LiCoO_2 used as the cathode exhibited a lower retention rate after 100 charge–discharge cycles [25]. Lithium foil is typically easy to trade with a reasonable price between 300 and $400 \text{ USD}\cdot\text{kg}^{-1}$. The cost for making the thinnest layer of lithium metal anode exceeds $1000 \text{ USD}\cdot\text{kg}^{-1}$. Subsequently, a very reactive lithium-metal anode with durable adhesion behavior requires complicated processing techniques and harsh operating conditions such as punching, rolling, deposition, and evaporation. Then, the price will increase significantly compared with currently available graphite

anodes [26–29]. Supposedly, the manufacturing of a thin layer of lithium-metal anode by the battery company will attract a much lower cost than purchasing Li foil from another provider [26]. The cost of Li-based material is about four times higher than it was 10 years ago because of the limited global reserves of lithium. Moreover, the extraction of lithium from seawater is costly and challenging. Li-metal anodes in batteries can be regarded as the Holy Grail in Li-metal batteries. The inconsistency with respect to lithium's energy density and safety issues has encouraged the design of anode-free batteries [30].

Anode-free batteries provide high volumetric energy density compared to Li-ion batteries with graphite anodes. Figure 2 shows the differences in battery configuration, resulting in a large improvement in volumetric and gravimetric energy density. Massive volume changes occur during the charge and discharge process in the cell stack of anode-free Li-ion batteries. For a volume expansion of approximately 20%, the stack's plating was assumed to exhibit negligible contraction on the cathode side, while a 57.1% increase in volumetric energy density was found for the Li-ion battery system [31].

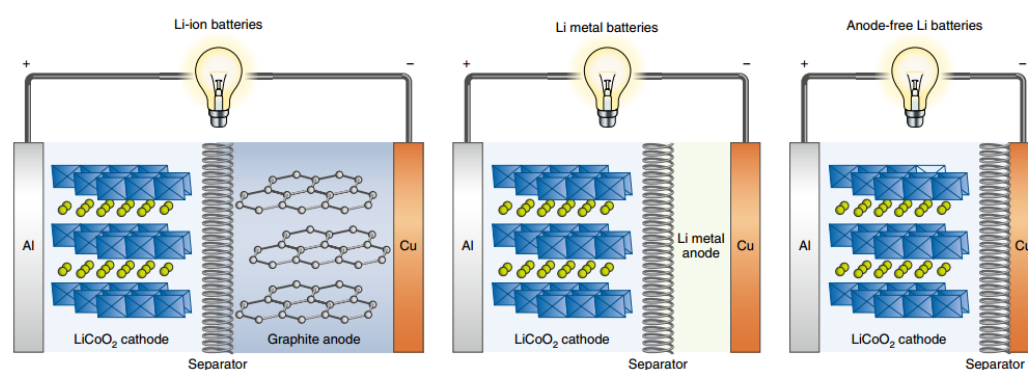


Figure 2. Differences in battery manufacturing and related improvement in volumetric and gravimetric energy density (adopted and modified from [31]).

Figure 2 describes the differences in the cell configuration, as well as the related improvement in both gravimetric and volumetric energy density. Furthermore, while preparing a thin film with $<100\ \mu\text{m}$ thickness, the uniform distribution of active material and the control of purity are challenging steps [30]. Today's LIBs are predominately based on intercalation chemistry, involving a graphitic carbon anode and a lithiated transition metal layered oxide cathode with the general formula LiMO_2 ($M = \text{Ni, Mn, or Co}$) [19]. Upon charging, the transition metal ion is oxidized (e.g., $\text{Ni}^{2+} \rightarrow \text{Ni}^{3+}$ or Ni^{4+}) as electrons and Li^+ ions are extracted. The Li ions then migrate and intercalate into the graphitic anode, which is accordingly reduced (see Figure 3a). Upon discharge, these processes are reversed. A major challenge with anode-free full cells is the large volume expansion of the cell stack that accompanies the plating and stripping of lithium. In the example system shown in Figure 3b, $6.2\ \text{mAh}\cdot\text{cm}^{-2}$ of plated lithium capacity corresponds to a $30\ \mu\text{m}$ increase in stack thickness or a volume expansion of nearly 20%. However, this is still an underestimate, as the actual thickness of the porous high-surface area of deposited lithium of a particular capacity would almost certainly exceed the theoretical value.

Further handling of a thin film is also challenging due to the lack of mechanical toughness, and it is also highly reactive with air and moisture. Henceforth, the lithium metal coating process with fewer effective layers or stabilizing interphases is relatively insignificant. Anode-free lithium-ion batteries come with many problems. The trivial changes in battery manufacturing, compared with existing Li-ion batteries, indicate that anode-free battery production is efficiently designed for the current battery configuration setup with slight modifications. In the meantime, anode-free LIBs are manufactured in completed discharge conditions, in which they experience a lower energy state. Moreover, anode-free Li-ion batteries are comparatively safer than Li-ion batteries.

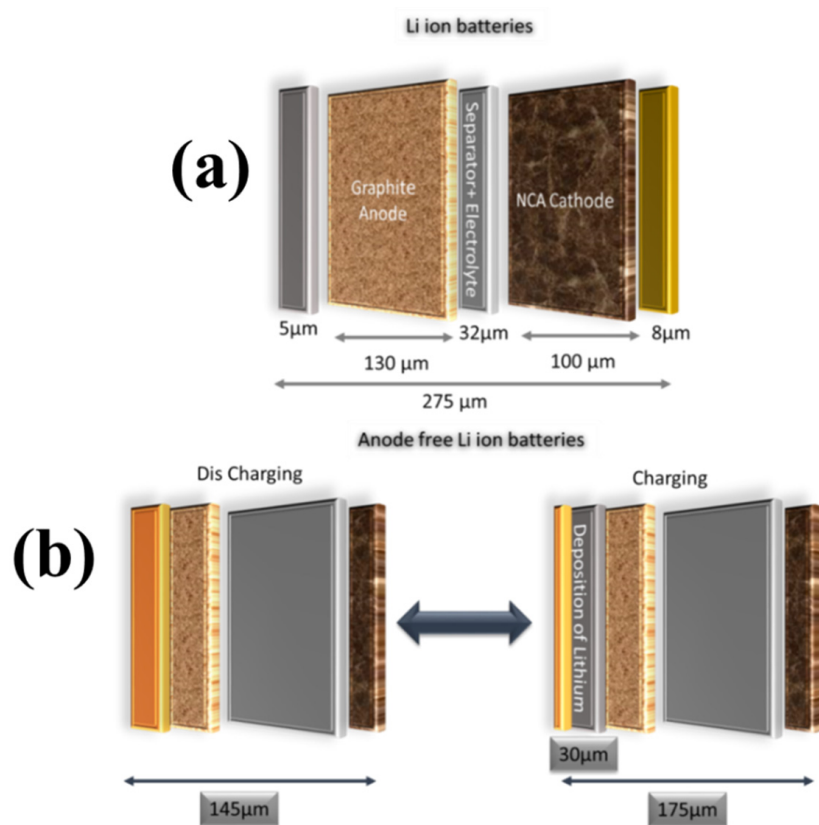


Figure 3. Schematic diagram of the loading of LIBs featuring an NCA (lithium–nickel–cobalt–aluminum oxide) cathode system with a thickness of 100 μm . **(a)** Schematic illustration of an example lithium-ion battery using an NCA cathode of thickness 100 μm and a loading of 30.5 $\text{mg}\cdot\text{cm}^{-2}$, drawn to scale. **(b)** Schematic illustration of an anode-free full cell using an equivalent NCA cathode, in both charged and discharged states. The difference in energy density can be clearly visualized. There is a $\sim 20\%$ volume change associated with the plating and stripping of lithium, which will have to be accommodated (modified from [30]).

The anode-free battery's typical structure is $\text{Cu}||\text{LiCoO}_2|\text{Al}$ (assuming LiCoO_2 as the positive electrode). During the first charge, lithium ions are separated from the positive lattice and deposited on the lithium metal's negative collector. The battery works like a lithium metal cell during the subsequent cycle, but the positive electrode only acts as the source of lithium. Compared with commercialized lithium-ion batteries, anode-free batteries simplify the slurry preparation and electrode coating, having the characteristics of easy assembly and low cost. Moreover, because there is no inert body, the volume of a negative electrode-free lithium-ion battery can be minimized, and it has a high energy density. The energy storage of the $\text{Cu}||\text{LiFePO}_4$ battery is over 40% higher than that of traditional lithium-ion batteries. Compared with traditional lithium-metal batteries, lithium metal is not used in the preparation and assembly process of non-negative lithium-metal batteries. The lithium used in the battery cycle is completely stored in the stable positive electrode with relatively higher safety. Furthermore, anode-free lithium metal batteries have another advantage; they can match lithium-containing cathode materials in terms of stable process performance, which greatly improves the prospect of industrialization.

However, there are still many challenges.

(1) The formation of "dead lithium" on the anode side: the binding force of lithium ions deposited on the surface of the current collector copper foil is weak, resulting in large contact resistance and mossy "dead lithium". The research of Zhang's group in the Argonne National Laboratory in the United States showed that only 23% of the lithium ions in $\text{Cu}||\text{LiNi}_{1/3}\text{Mn}_{1/3}\text{Co}_{1/3}\text{O}_2$ can return to the positive electrode of the NMC in the

discharge stage, while the remainder is “dead lithium”, which reduces the capacity of the battery.

(2) Lithium dendrite’s problems: similar to lithium metal batteries, lithium dendrite can easily grow on the negative side during charge and discharge. The existence of lithium dendrite not only brings potential safety hazards, but also increases the side reaction between lithium metal and electrolyte, causing rapid loss of lithium metal, resulting in low cycle efficiency of lithium and rapid attenuation of battery capacity, ultimately reducing the electrochemical performance of the lithium-free negative battery.

Therefore, there are key scientific and technical challenges that need to be addressed, e.g., fundamentally solving the nonuniform lithium deposition, reducing the “dead lithium”, effectively inhibiting the growth of lithium dendrite, and improving the safety performance and cycle stability of the battery while increasing the energy density.

3. Approaches for Enhancing the Performance of Anode-Free Batteries

Neudecker and his team reported the first study on anode-free lithium-ion batteries [28]. They used a thin film with 3 μm thick LiCoO_2 cathodes, a LiPON film as the electrolyte, and Cu sputter-deposited for the current collector. They applied $5 \text{ mA}\cdot\text{cm}^{-2}$ current to provide excellent cyclability, but the capacity was less than $0.1 \text{ mAh}\cdot\text{cm}^{-2}$ of lithium, which was plated. Review studies have mainly focused on the modification of anode-free lithium-ion batteries in the electrolyte and current collector; in addition to solid-state and anode-free batteries, anode-free sodium batteries and anode-free sulfur batteries have also been discussed.

In energy storage devices, monitoring and sustaining the lithium inventory are key factors for evaluating and improving its performance. In the last few years, the foremost aim of anode-free lithium-ion battery research was to improve energy density by investigating the irreversible loss of lithium inventory during charging and discharging. The optimization of the cathode is an essential factor to achieve higher electrochemical performance. Anode-free Li-ion batteries face some deficiencies, such as the decreasing capacity of lithium metal at the current collector. Many researchers are now focusing on the fast movement of ions through the electrolyte and confirming the solid electrolyte interphase that provides the superficial conductivity of Li ions and prevents the electrolyte decomposition on the surface of deposited lithium.

The important steps (as shown in Figure 4) for achieving an improved anode-free battery are as follows: (1) modification of the electrolyte; (2) current collector modification; (3) improvement of the manufacturing process and the cycling parameters to avoid capacity loss.



Figure 4. Framework indicating the three categories of strategies used to improve the performance of anode-free lithium-ion batteries (modified from [29]).

3.1. Electrolyte Modification

The role of electrolytes is essential and critical for anode-free lithium-ion batteries. Furthermore, they represent an essential element for defining the composition of the SEI layer and morphology of the lithium deposition on the lithium metal surface. The electrolyte enables a smooth and uniform deposition of lithium metal on the current collector,

constraining unwanted side reactions between the electrolyte and metallic lithium. Subsequently, the electrolyte can adjust itself and decay into a favorable SEI on the surface of the deposited lithium with high ionic conductivity to certify the electrochemical accessibility to the surrounded lithium metal and actual passivation to alleviate the additional decomposition of the electrolyte. Both of the above parameters are promising candidates for preserving lithium inventory over charge–discharge cycling.

Qian et al. reported influential work on anode-free lithium-ion batteries using liquid electrolytes [29], by investigating the tradeoff using an electrolyte of standard carbonate: ether-based, concentrated electrolyte, 4 M lithium bis-fluorosulfonyl imide in dimethoxyethene versus 1 M LiPF₆ in ethylene carbonate (EC)/dimethyl carbonate 1:2, *v/v*. The 1 M LiPF₆ used in the anode-free lithium-ion battery as electrolyte has a copper current collector. The LiFSI, which is added to dimethoxyethene electrolyte to stabilize the lithium metal cathode's plating and stripping, shows both enhanced deposition morphology and promising SEI layer formation. The electrolyte with high concentration provides up to 60% retention after 50 charge–discharge cycles, keeping an average CE higher than 99%. At a current speed of 0.2 mA·cm⁻², the starting lithium stripping capacity was 1.7 mAh·cm⁻² [17,19].

After initial investigations, a multitude of strategies were established by varying the material's concentration and composition used in the electrolyte solution and salt in anode-free lithium-ion batteries. Beyen et al. described the dual salt formulation that developed when using a high concentration of salt. They used 1 M lithium bis trifluoromethanesulfonyl imide and 2 M LiFSI in DME dioxolane with a ratio of 1:1 *v/v*. That experiment showed 50% capacity retention after 50 charge–discharge cycles in anode-free lithium-ion batteries [29].

Hagos and coworkers studied the use of carbonate-based electrolyte consisting of 2 M LiPF₆ in EC/diethyl carbonate (1:1 *v/v*) diluted by 50% volume with fluoroethylene. The electrolyte reported by Hagos et al. provided improved electrochemical performance with a wider potential window than the ether-based electrolyte. A large amount of fluorinated solvent stabilized the lithium deposition because of the rich SEI layer of LiF. In contrast, it reduced the overall amount of salt and the viscosity of the electrolyte compared to the high-concentration electrolyte. Anode-free lithium-ion batteries using the above electrolyte with a copper foil current collector were built, which still had 40% CE after 50 cycles [32]. From this reported work, we can conclude that the carbonated-based electrolyte plays an important role in providing higher specific capacity with a wide potential window in anode-free lithium batteries [33]. Weber and his group reported anode-free Cu | NMC lithium-ion batteries with dual salt carbonate-based electrolytes. The electrolyte consisted of 0.2 M LiBF₄ and 1 M lithium difluoro oxalato borate in a mixture of FEC/DEC (1:2 *v/v*). This electrolyte showed excellent improvement with 90% capacity retention after 50 cycles and 80% capacity retention after 90 cycles [34]. Substantial progress has been made in terms of modification regarding electrolytes in the last few years. An in-depth understanding of the importance of the SEI layer is yet to be achieved, because it can influence the lithium's stripping, plating, conductivity, electronic insulation, chemical passivation, mechanical stability, and interfacial energy.

3.2. Amendment of the Current Collector

The alteration of the current collector used for the deposition of lithium is another aspect for improving the cycle life of anode-free lithium batteries. It plays an important role in describing the consequent growth of the deposited lithium and initial nucleation condition. Consequently, it is crucial in the development of anode-free lithium-ion batteries. Pretreatment of the current collector can enhance the morphology of the deposition of lithium. A coating can be used as an artificial SEI layer to avoid the deposition of electrolyte on the deposited lithium.

A series of current collectors with coating films and artificial SEIs using polyethylene oxide were reported. The use of PEO could improve the retention rate when using the ether-

based electrolyte. The anode-free lithium batteries consisted of Cu@PEO || LFP, which provided 64% capacity retention after 50 cycles. For investigation in multilayer graphene, a wide-area current collector was used, which was relatively larger than the cathode area, to decrease the deposited lithium metal surface pressure. A coating of graphene oxide and garnet was able to moderately improve the electrochemical performance of the anode-free lithium batteries. The coating acted as an artificial SEI layer, preventing the deposited layer of Li from reacting with the carbonate-based electrolyte. Furthermore, in the presence of carbonated electrolytes, a coulombic efficiency in the range of 97% to 99% was achieved [19].

Moreover, there is an opportunity to improve the electrochemical performance of anode-free LIBs by modifying the current collector. Many groups used bare copper foil as the substrate for deposition. Thin layers of lithium and tin metal deposition substrate were also investigated in anode-free batteries [35,36]. These layers were deposited on the surface of copper foil. LiPF₆ electrolyte was used, exhibiting improved electrochemical performance in the tin coating with bare Cu foil. The cyclic performance was highly increased from 30 to 80 cycles, showing 30% capacity retention after 50 cycles.

The current collector plays a key role in determining the deposited lithium's morphology during battery operation; hence, its lithium inventory performance is essential in anode-free batteries. Many studies have been conducted on the pretreatment, coating, and modification of the current collector. However, there is still room for further research. The coating layer must be defect-free, tolerant, and robust before using the artificial SEI layer. The layer also needs higher volume changes of the deposited lithium metal during charge and discharge cycles. The lithiation factor should be controlled to enhance the ionization of the limited lithium inventory, which should be accessible for stripping and plating.

3.3. Optimization of Battery Manufacturing and Cycling Parameters

The final basis for sustaining the lithium inventory in anode-free lithium batteries is represented by the manufacturing of batteries and the cycle performance parameter used during the operation. The working conditions, such as operational controls, modified resting steps, application of temperature and pressure, and optimized first cycle protocol, can affect the energy storage device [37–40]. The initial manufacturing steps are essential for manufacturing a highly stable and passivating SEI layer on the anode side before extending the cycle life. As the anode-free LIBs already have the absence of an anode, optimal battery manufacturing approaches are different from other applied systems. It should be noted that optimizing the starting manufacturing process for anode-free LIBs is still a newly developing area of research.

Beyene and coworkers determined a new approach to a cycling and resting protocol for anode-free LIBs. When applying electrolyte at a high concentration, a more robust SEI layer was formed on the deposited lithium metal [41]. They used a method in which the lithium was deposited at a low current rate while the battery was charged. The battery was rested for 24 h after the first cycle to enable the formation of an SEI layer with rich fluorinated species made from LiFSI electrolyte.

Furthermore, when the battery was discharged at a high current rate, the deposited lithium was stripped away. It was concluded that the battery was galvanostatically cycled at up to 2 mA·cm⁻². Beyene and his coworkers claimed that the lithium deposition would become uniform and smooth with increasing temperature. When this method was used to prepare an anode-free Cu || LFP full battery, it provided stable cycling performance and a coulombic efficiency of up to 99%. After 50 cycles, it exhibited a charge the retention of up to 64%.

Louli and coworkers discussed the effects of mechanical stack pressure on the cyclic performance of anode-free LIBs [20]. They used anode-free Cu || NMC for a large area with a low amount of electrolyte of 3 g·Ah⁻¹. The cycling of Cu || NMC was further checked using a high pressure of up to 2200 kPa. The cyclic performance typically increased with pressure. Furthermore, the level of improvement in capacity retention depended on the type of electrolyte. Another research group also reported a new approach called

“hot formation”, in which the first two cycles were checked at a higher temperature of approximately 400 °C. They concluded that the cycle formation at a higher temperature enabled a denser and more uniform layer following lithium deposition, than at 200 °C. The formation on an optimized temperature approach was applied in an anode-free Cu || NMC full battery at a pressure of 75 kPa, showing 50% capacity retention after 100 cycles [41]. Even though the hot formation approach also generated gas in the battery, it was further used under high pressure (1200 kPa) with concentrated electrolyte salt FEC/DEC in the ratio of 1:2. Using this electrolyte, the anode-free LIBs showed 80% retention. The initial capacity of the device was 95% after 100 cycles. The starting lithium stripping capacity was $2.5 \text{ mA}\cdot\text{cm}^{-1}$ at the current rate of $0.5 \text{ mA}\cdot\text{cm}^{-2}$. This was a tremendous achievement in the field of electrochemistry, with respect to not only anode-free devices but also lithium-metal anodes. The use of an electrolyte mixture with a high salt concentration in anode-free batteries represented a landmark.

To improve the capacity retention and to enlarge the cycling ability, in 2020, a group introduced a new approach to study the NMR metrology of anode-free lithium metal batteries, where lithium is directly applied on the copper bare current collector and LiFePO_4 is used as the cathode. The metrology permits dead or inactive lithium formation when stripping and plating lithium in anode-free lithium-ion batteries. NMR could be used to measure the SEI and dead lithium formation, and their relative speed of formation was compared in ether and carbonate electrolytes. When using FEC as an additive, no dead Li was detected. The amount of Li metal was observed during rest time. The corrosion of Li was observed in carbonated and ether electrolytes.

Corrosion can also be observed when the battery is not in operation. The high speed of corrosion is accredited to the formation of SEI on both lithium and copper metal. The study showed that a polymer coating and a modification of the copper surface helped to stabilize the lithium metal surface [41].

4. Anode-Free Lithium–Sulfur Batteries

Lithium–sulfur batteries are perfect candidates for preparing next-generation batteries with higher energy density. The gravimetric capacities are $1675 \text{ mAh}\cdot\text{g}^{-1}$ for sulfur and $3861 \text{ mAh}\cdot\text{g}^{-1}$ Li. Sulfur is abundant and has low cost compared to other transition metals [42].

Sanjay Nanda and his coworkers reported an anode-free battery by combining $\text{Li}_2\text{S}/\text{CNT}$ used as the cathode material with bare Cu foil [41]. To the best of our knowledge, these reported lithium–sulfur batteries were the first anode-free batteries to be configured. They introduced tellurium (Te) into the Li–S batteries as the cathode material. Te enabled excellent improvement in the Li plating and stripping by establishing a sulfur-rich and tellurized electrolyte SEI layer on the Li surface. Tremendous progress was found in the cycle life of anode-free Li–S with lean electrolyte. Polysulfide reacts with Te to form soluble polytellurosulfides that shift to the anode side and generate the stable lithium thiotellurate and lithium telluride on the Li anode surface. This study showed that Te addition is a viable strategy to form a more stable deposition of Li, which can provide excellent electrochemical performance. This study provided a critical step to overcome the problem of short cyclability and energy density. Compared to the Li || Li_2S half-battery with a large amount of lithium, the anode-free Cu || Li_2S full battery highlighted the impact of small lithium inventory on electrochemical performance (Figure 5) [34].

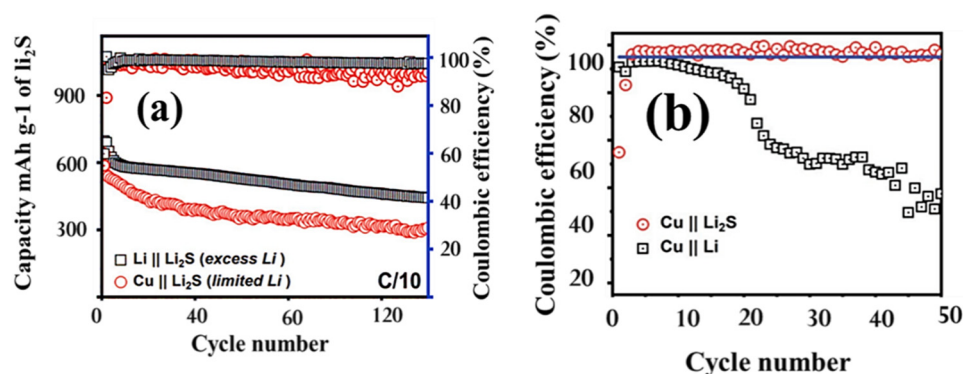


Figure 5. (a) Electrochemical performance of Li || Li₂S half battery and anode-free Cu || Li₂S battery, with a 4 mg·cm⁻² cathode. (b) Coulombic efficiencies of plating and stripping lithium on Cu foil from Li₂S cathode and lithium-metal counter electrode (modified and adopted from [42]).

5. Anode-Free Sodium Batteries

In various energy storage devices, sodium is a more promising alternative than lithium due to its unique properties such as higher gravimetric capacity (1165 mAh·g⁻¹) and lower redox potential (−2.71 V). Furthermore, sodium is available in high abundance in the earth's crust and is cheaper than lithium [43,44]. The use of sodium instead of lithium also exhibits many advantages, especially in cobalt-free sodium-ion batteries. In sodium-ion batteries, the copper can be replaced with easily available materials that are lightweight, cheaper, more flame-resist, and environmentally friendly compared to lithium-ion batteries [44,45]. Using sodium as the cathode material facilitates the absence of an appropriate anode host material with lower redox potential and decent cycle ability [46,47]. Additionally, using metallic sodium can help to overcome this problem.

However, sodium metal is highly reactive with moisture and air, sometimes more reactive than lithium. In most cases, it would be a disadvantage to form a full battery without free sodium metal. We can design an anode-free sodium battery by pairing a completed sodiated cathode with the current collector for sodium plating and stripping. This can provide excellent energy density and solve the abovementioned problems [48].

As with the lithium metal anode, the sodium metal anode also suffers from various issues. Due to the deposition of sodium metal, reactive porous mossy deposits on high-surface-area materials can decrease the stripping and plating effect. Sodium metal has not received much attention for its improvements in this regard. Furthermore, the proposed solutions for improving the coulombic efficiency of sodium-ion batteries are similar to those for lithium metal batteries, such as optimizing electrolytes, controlling the layer's thickness to homogenize the Na ion flux, and modifying the current collector.

Nevertheless, there are significant differences between lithium and sodium's physical and chemical properties, such that the deposition of sodium cannot be considered similar to that of lithium. Sodium ions (116 pm) are more extensive than lithium ions (96 pm). Nevertheless, sodium ion is less polarizing because of its lower charge density. Lithium metal is a stronger reducing agent than sodium, and the melting point of sodium (98 °C) is much lower than that of lithium (181 °C).

Cohn et al. reported in 2017 an anode-free sodium-ion battery using a sodiated iron pyrite cathode combined with a thin layer of a carbon-coated aluminum foil [49]. The thin layer of carbon exhibited a low sodiation capacity of 0.05 mA·cm⁻². In this study, they described the challenges of energy density faced by sodium metal batteries. These challenges can be solved by introducing an anode-free configuration that can enable the utilization of the nanocarbon nucleation layer formed on Al current collectors.

This configuration showed excellent electrochemical performance, high stability, and more efficient plating and stripping of sodium metal on applied ranges up to 4 mA·cm⁻². The obtained sample showed a long cycle life of up to 10,000 cycles at the current rate of 0.5 mA·cm⁻² with long-term stability. The electrode was checked by SEM at different time

intervals, as shown in Figure 6. From the SEM images, we can observe the progress from the seeding of well-formed sodium to the formation of a shiny, smooth sodium metal with a uniform hexagonal morphology.

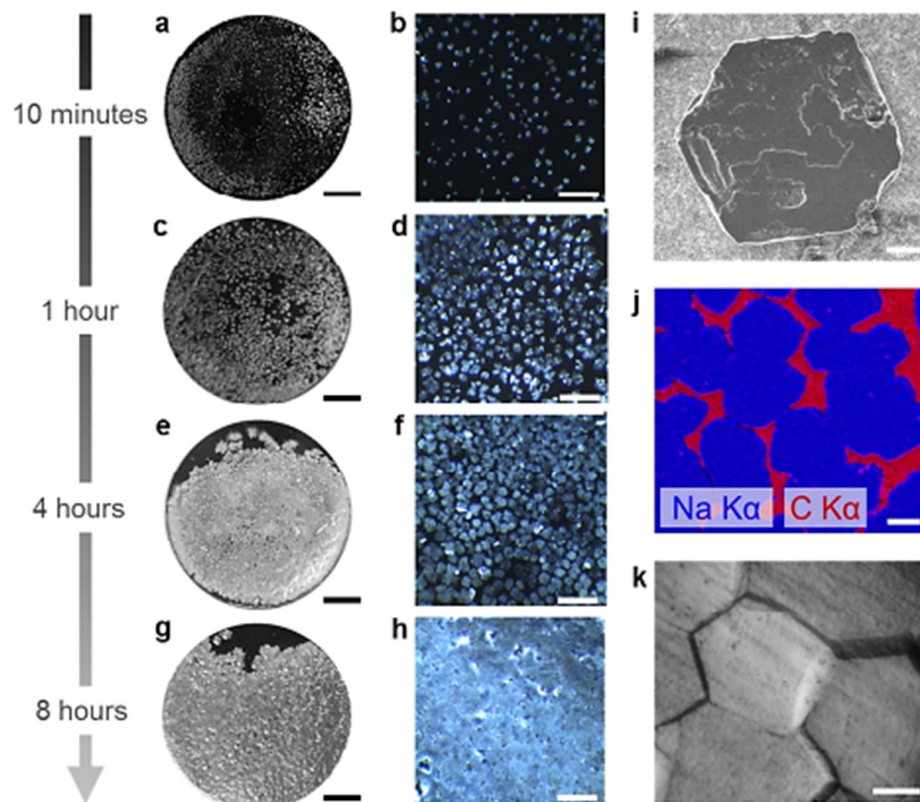


Figure 6. SEM images of sodium metal on carbon/Al electrodes following plating at $0.5 \text{ mA}\cdot\text{cm}^{-2}$ after (a,b) 10 min, (c,d) 1 h, (e,f) 4 h, and (g,h) 8 h. (i) SEM image of hexagon-shaped sodium metal island (SB = $20 \mu\text{m}$). (j) EDS map showing coalescing sodium metal islands (CB = $50 \mu\text{m}$). (k) Micrograph of plated sodium metal film with $4 \text{ mAh}/\text{cm}^2$ loading (SB = $20 \mu\text{m}$) (adopted with [49]; copyright (2006) American Chemical Society).

6. Anode-Free Solid-State Batteries

The various fundamental limitations of lithium metal batteries were widely discussed in this review paper, such as the many types of liquid electrolytes, modification of the current collector, battery manufacturing optimization, and cycling parameter optimization. Those limitations have led to extensive interest in all-solid-state batteries [49,50]. By inhibiting lithium dendrite growth, the risk of the battery's internal shorting and the consequent thermal runaway can be removed when using the solid-state electrolyte [51,52]. The energy density can be improved by skipping the polymer separator, using as little electrolyte as possible compared to liquid electrolytes [48]. Greater improvements in the electrochemical performance and energy density were observed when using a solid-state electrolyte. The solid-state electrolyte also showed a limited gas evolution as compared to liquid electrolyte [52].

Despite the above merits, the improvement of solid-state lithium-metal batteries faces many difficulties. At room temperature, the traditional solid-state electrolyte suffers from relatively poor ionic conductivity. Optimized SSE materials such as LIPON, LATP, LAGP, NASICON, and garnet type LLZO feature lower ionic conductivity than their liquid electrolyte counterparts [51–53].

Solid-state electrolytes are commonly divided into three categories: inorganic electrolytes, organic polymer electrolytes, and ceramic polymer composite electrolytes.

For rigid batteries, inorganic electrolytes are more suitable as they can work in a harsh environment. They show high elasticity, perfect chemical/thermal stability, low electronic conductivity, high ionic conductivity, and high electrochemical potential. [54–61]. On the other hand, solid polymer electrolytes can enable many geometries, high flexibility, and cost-effectiveness for commercialization. However, the ionic conductivity of polymer electrolytes is much lower than that of inorganic solid electrolytes [62–65]. Featuring the advantages of inorganic solid electrolytes and organic polymer electrolytes, improved thermal and chemical stability and enhanced mechanical properties can be obtained when using ceramic polymer composite electrolytes [66–70].

Lee and his coworkers reported an anode-free solid-state battery featuring a $\text{LiNi}_{0.90}\text{Co}_{0.05}\text{Mn}_{0.05}\text{O}_2$ cathode with $\text{Li}_6\text{PS}_5\text{Cl}$ sulfide solid electrolyte [70]. The layer of solid electrolyte was consistently used on the cathode and pressed with the warm pressing machine. The cathode was covered by a thin layer of $\text{Li}_2\text{O}-\text{ZrO}_2$ to maintain the stability of the solid electrolyte. The anode nanocomposite with a thickness of 5 μm consisted of lithiophilic gold (Ag) nanoparticles and carbon black as the buffer layer between the stainless-steel current collector and solid electrolyte. The nanocomposite buffer allowed obtaining dense and dendrite-free lithium. The uniform deposition on the current collector acted as stable interface between solid electrolytes and lithium metal. The obtained anode-free battery provided $6.8 \text{ mAh}\cdot\text{cm}^{-2}$ capacity with an applied current density of 0.5 C. The test for 10,000 cycles showed 99.98 % retention, which is approximately similar to the coulombic efficiency of industrialized Li-ion batteries using a graphite anode.

Current electric vehicles can drive up to 400 km. However, the range of electric vehicles can be extended by more than 280 km while maintaining the same energy cost it a battery with a 60% volumetric capacity is implemented [71].

When comparing both types of batteries, it can be concluded that they both use $\text{Li}(\text{Ni}_{0.5}\text{Mn}_{0.3}\text{Co}_{0.2})$ as the cathode, but the anode-free batteries store charge as electroplated lithium metal instead of using a graphite host. Thus, 100% of the lithium comes from the positive electrode because the anode-free batteries use zero excess lithium [72,73].

Weber and coworkers reported anode-free batteries with a long life cycle by using dual salt carbonated electrolyte. Cells with a dual salt $\text{LiDFOB} + \text{LiBF}_4$ electrolyte had the best performance among all the electrolytes tested, providing 80% capacity after 90 cycles, which is the longest life demonstrated to date for cells with zero excess lithium [74].

A further merit of anode-free batteries is their superior energy density retention to Li-ion batteries. Figure 7 provides a comparison of anode-free and Li-ion cells with different electrolytes. Lithium difluoroxyalate electrolyte provided a higher energy density than the optimized Li-ion battery for 120 cycles. The authors characterized the degradation of anode-free batteries with LiDFOB and LiBF_4 electrolytes. Using scanning electron microscopy and X-ray, they observed the deterioration of the starting pristine lithium morphology. Furthermore, they observed the depletion of electrolyte with increasing lithium porosity by using ultra sonic transmission mapping. To address safety concerns, they measured the battery's temperature during charging and compared it with another battery reported in the literature that used a different electrolyte. They found that the optimized electrolyte extended the anode-free battery life up to 200 cycles.

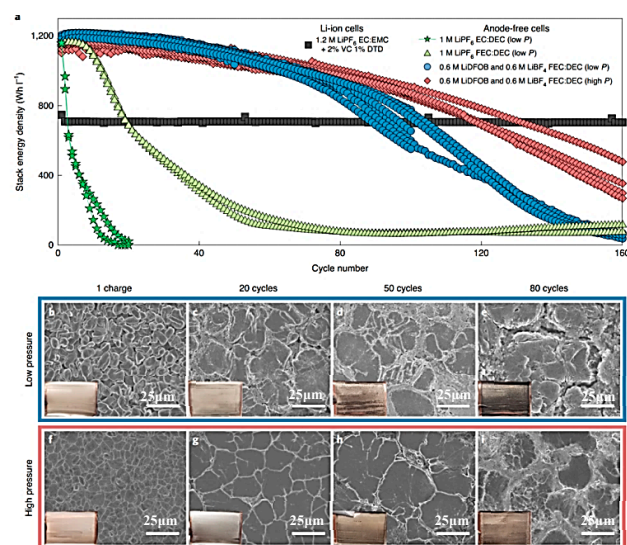


Figure 7. (a) Comparison of anode-free and Li-ion cells with different electrolytes. (b–i) SEM images of plated lithium at different pressure after different charging cycles. Scale bars 25 μm [74].

7. Conclusions

In summary, anode-free batteries have gained tremendous attention in recent years. Anode-free batteries contain a particular prototype of a current collector, featuring an optimized electrolyte with a separator and cathode current collector. They provide high energy density, improved safety, and cost-effective and simple battery assembly. As compared to traditional lithium/sodium–sulfur batteries, anode-free lithium batteries possess a limited lithium source and exhibit excellent electrochemical performance with a long cycle life. However, lithium metal may be consumed during plating and stripping via an irreversible reaction involving electrolyte and metal. As a result of the irreversible reaction, dead lithium metal is formed. The cycle life is affected by this dead lithium. To solve this problem, several techniques have been developed, and we reported them in this paper. We summarized the significant challenges and fundamental issues. For example, optimizing the anode-side current collector, implementing a liquid electrolyte, and improving the cyclic performance and assembly of batteries can increase the LIRR value (99.99%) to enable industrial applications. A clear understanding of the role of SEI layer on the lithium surface, as well as its individual components, is necessary for the development of optimized electrolyte formulations. To improve the cycle life of anode-free batteries, the formation of high-ionic-conductivity interfacial species such as Li_3PS_4 and high-surface-energy interfacial species such as LiF is especially effective. Furthermore, mixed polysulfide additives and fluorinated electrolytes combine the high wettability of common electrolytes and low viscosity for anode-free lithium-ion batteries. Modifying the anode-side current collector with lithophilic materials is also a useful approach for improving the lithium deposition's reversibility. We investigated and summarized enhanced mechanisms from the perspectives of the electrolyte, current collector, and protocol. Although tremendous progress has been achieved, there are still several remaining tasks that need to be addressed.

The poor capacity retention is a difficult challenge for anode-free batteries, resulting in electrodeposition of metal at the poorly organized interface between the electrolyte and current collector. There are two ways to solve this problem: (1) evaporation and spin-coating of organic polymers can provide better contact between anode materials and current collectors; (2) high-conductivity self-supporting materials directly used as the negative electrode can negate the need for current collectors. Certainly, the combination of modification techniques with respect to the electrolyte, current collector, and cathode will be the most important solution for future anode-free batteries. By using advanced devices and techniques, we can better study the internal mechanism underlying the movement

of ions during charging and discharging in anode-free batteries. We believe that our review paper can provide a deep understanding of anode-free batteries, as well as enhance their development.

Author Contributions: Conceptualization, J.Z. and A.K.; methodology, X.L. and Y.L.; software, S.D., formal, L.L.; validation, H.Z. and D.L. All authors have read and agreed to the published version of the manuscript.

Funding: This research was funded by Special Funds for the Science and Technology Innovation Project of Guangdong Provincial Department of Education (grant number 2021KTSCX278) and the Shenzhen Government's Plan of Science and Technology (JCYJ20220811141844002).

Institutional Review Board Statement: Not applicable.

Informed Consent Statement: Not applicable.

Data Availability Statement: Not applicable.

Conflicts of Interest: The authors declare no conflict of interest.

References

1. Manthiram, A. A reflection on lithium-ion battery cathode chemistry. *Nat. Commun.* **2020**, *11*, 1–9. [[CrossRef](#)] [[PubMed](#)]
2. Shao, A.; Tang, X.Y.; Zhang, M.; Bai, M.; Ma, Y. Challenges, Strategies, and Prospects of the Anode-Free Lithium Metal Batteries. *Adv. Energy Sustain. Res.* **2022**, *4*, 2100197. [[CrossRef](#)]
3. Thackeray, M.M.; Wolverton, C.; Isaacs, E.D. Electrical energy storage for transportation—Approaching the limits of, and going beyond, lithium-ion batteries. *Energy Environ. Sci. EES* **2012**, *5*, 7854–7863. [[CrossRef](#)]
4. Bruce, P.G.; Hardwick, L.J.; Abraham, K.M. Lithium-air and lithium-sulfur batteries. *MRS Bull.* **2011**, *36*, 506–512. [[CrossRef](#)]
5. Yuan, W.; Li, Y.; Ding, T.; Zhang, L.; Shu, J. Dendrite-free NaK alloy Anodes: Electrodes preparation and interfacial reaction. *Chem. Eng. J.* **2022**, *432*, 134353. [[CrossRef](#)]
6. Li, W.; Erickson, E.M.; Manthiram, A. High-nickel layered oxide cathodes for lithium-based automotive batteries. *Nat. Energy* **2020**, *5*, 26–34. [[CrossRef](#)]
7. Su, L.S.; Charalambous, H.; Cuia, Z.; Manthiram, A. High-efficiency, anode-free lithium-metal batteries with a close-packed homogeneous lithium morphology. *Energy Environ. Sci.* **2022**, *2*, 2648.
8. Xu, J.; Lin, F.; Doeff, M.M.; Tong, W. A review of Ni-based layered oxides for rechargeable Li-ion batteries. *J. Mater. Chem. A Mater. Energy Sustain.* **2017**, *5*, 874–901. [[CrossRef](#)]
9. Chae, S.; Choi, S.-H.; Kim, N.; Sung, J.; Cho, J. Integration of graphite and silicon anodes for the commercialization of high-energy lithium-ion batteries. *Angew. Chem.* **2020**, *59*, 110–135. [[CrossRef](#)] [[PubMed](#)]
10. Wu, J.; Cao, Y.; Zhao, H.; Mao, J.; Guo, Z. The critical role of carbon in marrying silicon and graphite anodes for high-energy lithium-ion batteries. *Carbon Energy* **2019**, *1*, 57–76. [[CrossRef](#)]
11. Cheng, X.-B.; Zhang, R.; Zhao, C.-Z.; Zhang, Q. Toward safe lithium metal anode in rechargeable batteries: A review. *Chem. Rev.* **2017**, *117*, 10403–10473. [[CrossRef](#)]
12. Kwon, H.; Lee, J.H.; Roh, L.; Baek, J.; Shin, D.J.; Yoon, J.K.; Ha, H.J.; Kim, J.Y.; Kim, H.-T. An electron-deficient carbon current collector for anode-free Li-metal batteries. *Nat. Commun.* **2021**, *12*, 5537. [[CrossRef](#)]
13. Lin, D.; Liu, Y.; Cui, Y. Reviving the lithium metal anode for high-energy batteries. *Nat. Nanotechnol.* **2017**, *12*, 194–206. [[CrossRef](#)] [[PubMed](#)]
14. Fang, C.; Wang, X.; Meng, Y.S. Key issues hindering a practical lithium-metal anode. *Trends Chem.* **2019**, *1*, 152–158. [[CrossRef](#)]
15. Wang, L.; Song, X.; Hu, Y.; Yan, W.; Tie, Z.; Jin, Z. Initial-anode-free aluminum ion batteries: In-depth monitoring and mechanism studies. *Energy Storage Mater.* **2022**, *44*, 461–468. [[CrossRef](#)]
16. Bai, P.; Li, J.; Brushett, F.R.; Bazant, M.Z. Transition of lithium growth mechanisms in liquid electrolytes. *Energy Environ. Sci. EES.* **2016**, *9*, 3221–3229. [[CrossRef](#)]
17. Xiang, J.; Yang, L.; Yuan, L.; Yuan, K.; Zhang, Y.; Huang, Y.; Lin, J.; Pan, F.; Huang, Y. Alkali-metal anodes: From lab to market. *Joule* **2019**, *3*, 2334–2363. [[CrossRef](#)]
18. Wang, H.; Liu, Y.; Li, Y.; Cui, Y. Lithium metal anode materials design: Interphase and host. *Electrochem. Energy Rev.* **2019**, *2*, 509–517. [[CrossRef](#)]
19. Yang, H.; Guo, C.; Naveed, A.; Lei, J.; Yang, J.; Nuli, Y.; Wang, J. Recent progress and perspective on lithium metal anode protection. *Energy Storage Mater.* **2018**, *1*, 199–221. [[CrossRef](#)]
20. Li, H. Practical evaluation of Li-ion batteries. *Joule* **2019**, *3*, 911–914. [[CrossRef](#)]
21. Louli, A.J.; Genovese, M.; Weber, R.; Hames, S.G.; Logan, E.R.; Dahn, J.R. Exploring the impact of mechanical pressure on the performance of anode-free lithium metal cells. *J. Electrochem. Soc.* **2019**, *166*, A1291–A1299. [[CrossRef](#)]

22. Yu, L.; Chen, S.; Lee, H.; Zhang, L.; Engelhard, M.H.; Li, Q.; Jiao, S.; Liu, J.; Xu, W.; Zhang, J.-G. A localized high-concentration electrolyte with optimized solvents and lithium difluoro (oxalate) borate additive for stable lithium metal batteries. *ACS Energy Lett.* **2018**, *3*, 2059–2067. [[CrossRef](#)]
23. Xie, Z.; Wu, Z.; An, X.; Yue, X.; Yoshida, A.; Du, X.; Hao, X.; Abudula, A.; Guan, G. 2-Fluoropyridine: A novel electrolyte additive for lithium metal batteries with high areal capacity as well as high cycling stability. *Chem. Eng. J.* **2020**, *393*, 124789. [[CrossRef](#)]
24. Albertus, P.; Babinec, S.; Litzelman, S.; Newman, A. Status and challenges in enabling the lithium metal electrode for high-energy and low-cost rechargeable batteries. *Nat. Energy* **2018**, *3*, 16–21. [[CrossRef](#)]
25. Zhang, W.; Wu, Q.; Huang, J.; Fan, L.; Shen, Z.; He, Y.; Feng, Q.; Zhu, G.; Lu, Y. Colossal Granular Lithium Deposits Enabled by the Grain-Coarsening Effect for High-Efficiency Lithium Metal Full Batteries. *Adv. Mater.* **2020**, *32*, 2001740. [[CrossRef](#)]
26. Hong, D.; Choi, Y.; Ryu, J.; Mun, J.; Choi, W.; Park, M.; Lee, Y.; Choi, N.; Lee, G.; Kim, B.-S.; et al. Homogeneous Li deposition through the control of carbon dot-assisted Li-dendrite morphology for high-performance Li-metal batteries. *J. Mater. Chem. A Mater. Energy Sustain.* **2019**, *7*, 20325–20334. [[CrossRef](#)]
27. Schmuck, R.; Wagner, R.; Horpel, G.; Placke, T.; Winter, M. Performance and cost of materials for lithium-based rechargeable automotive batteries. *Nat. Energy* **2018**, *3*, 267–278. [[CrossRef](#)]
28. Ryou, M.H.; Lee, Y.M.; Lee, Y.; Winter, M.; Bieker, P. Mechanical surface modification of lithium metal: Towards improved Li metal anode performance by directed Li plating. *Adv. Funct. Mater.* **2015**, *25*, 834–841. [[CrossRef](#)]
29. Niu, C.; Lee, H.; Chen, S.; Li, Q.; Du, J.; Xu, W.; Zhang, J.-G.; Whitting, M.S.; Xiao, J.; Liu, J. High-energy lithium metal pouch cells with limited anode swelling and long stable cycles. *Nat. Energy* **2019**, *4*, 551–559. [[CrossRef](#)]
30. Betz, J.; Bieker, G.; Meister, P.; Placke, T.; Winter, M.; Schmuck, R. Theoretical versus Practical Energy: A Plea for More Transparency in the Energy Calculation of Different Rechargeable Battery Systems. *Adv. Energy Mater.* **2019**, *9*, 1803170. [[CrossRef](#)]
31. Zhang, J.G. Anode-less. *Nat. Energy* **2019**, *4*, 637–638. [[CrossRef](#)]
32. Qian, J.; Adams, B.D.; Zheng, J.; Xu, W.; Henderson, W.A.; Wang, J.; Bowden, M.E.; Xu, S.; Hu, J.; Zhang, J.-G. Anode-free rechargeable lithium metal batteries. *Adv. Funct. Mater.* **2016**, *26*, 7094–7102. [[CrossRef](#)]
33. Mashtalir, O.; Nguyen, M.; Bodoian, E.; Swonger, L.; O'Brien, S.P. High-purity lithium metal films from aqueous mineral solutions. *ACS Omega* **2018**, *3*, 181–187. [[CrossRef](#)] [[PubMed](#)]
34. Becking, J.; Grobmeyer, A.; Kolek, M.; Rodehorst, U.; Schulze, S.; Winter, M.; Bieker, P.; Stan, M.C. Lithium-Metal Foil Surface Modification: An Effective Method to Improve the Cycling Performance of Lithium-Metal Batteries. *Adv. Mater. Interfaces* **2017**, *4*, 1700166. [[CrossRef](#)]
35. Hagos, T.T.; Thirumalraj, B.; Huang, C.-J.; Abrha, L.H.; Hagos, T.M.; Berhe, G.B.; Bezabh, H.K.; Cherng, J.; Chiu, S.-F.; Su, W.-N.; et al. Locally concentrated LiPF₆ in a carbonate-based electrolyte with fluoroethylene carbonate as a diluent for anode-free lithium metal batteries. *ACS Appl. Mater. Interfaces* **2019**, *11*, 9955–9963. [[CrossRef](#)]
36. Borodin, O.; Self, J.; Persson, K.A.; Wang, C.; Xu, K. Uncharted Waters: Super-Concentrated Electrolytes. *Joule* **2020**, *4*, 69–100. [[CrossRef](#)]
37. Beyene, T.T.; Bezabh, H.K.; Weret, M.A.; Hagos, T.M.; Huang, C.-J.; Wang, C.-H.; Su, W.-N.; Dai, H.; Hwang, B.-J. Concentrated dual-salt electrolyte to stabilize Li metal and increase cycle life of anode free li-metal batteries. *J. Electrochem. Soc.* **2019**, *166*, A1501. [[CrossRef](#)]
38. Yu, Z.; Wang, H.; Kong, X.; Huang, W.; Tsao, Y.; Mackanic, D.G.; Wang, K.; Wang, X.; Huang, W.; Choudhury, S.; et al. Molecular design for electrolyte solvents enabling energy-dense and long-cycling lithium metal batteries. *Nat. Energy* **2020**, *5*, 526–533. [[CrossRef](#)]
39. Zhang, S.; Fan, X.; Wang, C. An in-situ enabled lithium metal battery by plating lithium on a copper current collector. *Electrochem. Commun.* **2018**, *89*, 23–26. [[CrossRef](#)]
40. Pande, V.; Viswanathan, V. Computational screening of current collectors for enabling anode-free lithium metal batteries. *ACS Energy Lett.* **2019**, *4*, 2952–2959. [[CrossRef](#)]
41. Belt, J.R.; Ho, C.D.; Miller, T.J.; Habid, M.A.; Duong, T.Q. The effect of temperature on capacity and power in cycled lithium ion batteries. *J. Power Sources* **2005**, *142*, 354–360. [[CrossRef](#)]
42. Beyene, T.T.; Jote, B.A.; Wondimkun, Z.T.; Olbassa, B.W.; Huang, C.-J.; Thirumalraj, B.; Wang, C.-H.; Su, W.-N.; Dai, H.; Hwang, B.-J. Effects of concentrated salt and resting protocol on solid electrolyte interface formation for improved cycle stability of anode-free lithium metal batteries. *ACS Appl. Mater. Interfaces* **2019**, *11*, 31962–31971. [[CrossRef](#)]
43. Nanda, S.; Gupta, A.; Manthiram, A. Anode-Free Full Cells: A Pathway to High-Energy Density Lithium-Metal Batteries. *Adv. Energy Mater.* **2021**, *11*, 2000804. [[CrossRef](#)]
44. Gunnarsdóttir, A.B.; Amanchukwu, C.V.; Menkin, S.; Grey, C.P. Noninvasive In Situ NMR Study of “Dead Lithium” Formation and Lithium Corrosion in Full-Cell Lithium Metal Batteries. *J. Am. Chem. Soc.* **2020**, *142*, 20814–20827. [[CrossRef](#)] [[PubMed](#)]
45. Sun, B.; Xiong, P.; Maitra, U.; Langsdorf, D.; Yan, K.; Wang, C.; Janek, J.; Schroder, D.; Wang, G. Design Strategies to Enable the Efficient Use of Sodium Metal Anodes in High-Energy Batteries. *Adv. Mater.* **2020**, *32*, 1903891. [[CrossRef](#)] [[PubMed](#)]
46. Zheng, X.; Bommier, C.; Luo, W.; Jiang, L.; Hao, Y.; Huang, Y. Sodium metal anodes for room-temperature sodium-ion batteries: Applications, challenges and solutions. *Energy Storage Mater.* **2019**, *16*, 6–23. [[CrossRef](#)]
47. Zhang, W.; Zhang, F.; Ming, F.; Alshareef, H.N. Sodium-ion battery anodes: Status and future trends. *EnergyChem* **2019**, *1*, 100012. [[CrossRef](#)]

48. Kim, D.-Y.; Kim, D.-H.; Kim, S.-H.; Lee, E.-K.; Park, S.-K.; Lee, J.-W.; Yun, Y.-S.; Choi, S.-Y.; Kang, J. Nano hard carbon anodes for sodium-ion batteries. *Nanomaterials* **2019**, *9*, 793. [\[CrossRef\]](#)
49. Cohn, A.P.; Muralidharan, N.; Carter, R.; Share, K.; Pint, C.L. Anode-free sodium battery through in situ plating of sodium metal. *Nano Lett.* **2017**, *17*, 1296–1301. [\[CrossRef\]](#) [\[PubMed\]](#)
50. Viallet, V.; Seznec, V.; Hayashi, A.; Tatsumisago, M.; Pradel, A. Glasses and Glass-Ceramics for Solid-State Battery Applications. In *Springer Handbook of Glass*; Springer: Cham, Switzerland, 2019; pp. 1697–1754.
51. Schnell, J.; Gunther, T.; Knoche, T.; Vieider, C.; Kohler, L.; Just, A.; Keller, M.; Passerini, S.; Reinhart, G. All-solid-state lithium-ion and lithium metal batteries—paving the way to large-scale production. *J. Power Sources* **2018**, *382*, 160–175. [\[CrossRef\]](#)
52. Xia, S.; Wu, S.; Zhang, Z.; Cui, Y.; Liu, W. Practical challenges and future perspectives of all-solid-state lithium-metal batteries. *Chem* **2019**, *5*, 753–785. [\[CrossRef\]](#)
53. Manthiram, A.; Yu, X.; Wang, S. Lithium battery chemistries enabled by solid-state electrolytes. *Nat. Rev. Mater.* **2017**, *2*, 1–16. [\[CrossRef\]](#)
54. Zhao, W.; Yi, J.; He, P.; Zhou, H. Solid-state electrolytes for lithium-ion batteries: Fundamentals, challenges and perspectives. *Electrochem. Energy Rev.* **2019**, *2*, 574–605. [\[CrossRef\]](#)
55. Zheng, F.; Kotobuki, M.; Song, S.; Lai, M.O.; Lu, L. Review on solid electrolytes for all-solid-state lithium-ion batteries. *J. Power Sources* **2018**, *389*, 198–213. [\[CrossRef\]](#)
56. Sun, Y.-Z.; Huang, J.-Q.; Zhao, C.-Z.; Zhang, Q. A review of solid electrolytes for safe lithium-sulfur batteries. *Sci. China Chem.* **2017**, *60*, 1508–1526. [\[CrossRef\]](#)
57. Hayashi, A.; Noi, K.; Sakuda, A.; Tatsumisago, M. Superionic glass-ceramic electrolytes for room-temperature rechargeable sodium batteries. *Nat. Commun.* **2012**, *3*, 1–5. [\[CrossRef\]](#)
58. Kim, J.-J.; Yoon, K.; Park, I.; Kang, K. Progress in the Development of Sodium-Ion Solid Electrolytes. *Small Methods* **2017**, *1*, 1700219. [\[CrossRef\]](#)
59. Oudenhoven, J.F.M.; Baggetto, L.; Notten, P.H.L. All-solid-state lithium-ion microbatteries: A review of various three-dimensional concepts. *Adv. Energy Mater.* **2011**, *1*, 10–33. [\[CrossRef\]](#)
60. Guin, M.; Tietz, F.; Guillon, O. New promising NASICON material as solid electrolyte for sodium-ion batteries: Correlation between composition, crystal structure and ionic conductivity of $\text{Na}_3+\text{xSc}_2\text{SixP}_3-\text{xO}_{12}$. *Solid State* **2016**, *293*, 18–26. [\[CrossRef\]](#)
61. Anantharamulu, N.; Rao, K.K.; Rambabu, G.; Kumar, B.V.; Radha, V.; Vithal, M. A wide-ranging review on Nasicon type materials. *J. Mater. Sci.* **2011**, *46*, 2821–2837. [\[CrossRef\]](#)
62. Guin, M.; Tietz, F. Survey of the transport properties of sodium superionic conductor materials for use in sodium batteries. *J. Power Sources* **2015**, *273*, 1056–1064. [\[CrossRef\]](#)
63. Zhang, Z.; Zhang, Q.; Shi, J.; Chu, Y.S.; Yu, X.; Xu, K.; Ge, M.; Yan, H.; Li, W.; Gu, L.; et al. A Self-Forming Composite Electrolyte for Solid-State Sodium Battery with Ultralong Cycle Life. *Adv. Energy Mater.* **2017**, *7*, 1601196. [\[CrossRef\]](#)
64. Villaluenga, I.; Bogle, X.; Greenbaum, S.; Rojo, T.; Armand, M. Cation only conduction in new polymer– SiO_2 nanohybrids: Na^+ electrolytes. *J. Mater. Chem. A* **2013**, *1*, 8348–8352. [\[CrossRef\]](#)
65. Patel, M.; Chandrappa, K.G.; Bhattacharyya, A.J. Increasing ionic conductivity of polymer–sodium salt complex by addition of a non-ionic plastic crystal. *Solid State Ion.* **2010**, *181*, 844–848. [\[CrossRef\]](#)
66. Colò, F.; Bella, F.; Nair, J.R.; Destro, M.; Gerbaldi, C. Cellulose-based novel hybrid polymer electrolytes for green and efficient Na-ion batteries. *Electrochim. Acta* **2015**, *174*, 185–190. [\[CrossRef\]](#)
67. Kumar, K.K.; Ravi, M.; Pavani, Y.; Bhavani, S.; Sharma, A.K.; Rao, V.V.R.N. Investigations on the effect of complexation of NaF salt with polymer blend (PEO/PVP) electrolytes on ionic conductivity and optical energy band gaps. *Phys. B Condens. Matter* **2011**, *406*, 1706–1712. [\[CrossRef\]](#)
68. Zhang, Z.; Zhang, Q.; Ren, C.; Luo, F.; Ma, Q.; Hu, Y.-S.; Zhou, Z.; Li, H.; Huang, X.; Chen, L. A ceramic/polymer composite solid electrolyte for sodium batteries. *J. Mater. Chem. A* **2016**, *4*, 15823–15828. [\[CrossRef\]](#)
69. Ni'mah, Y.L.; Chen, M.-Y.; Cheng, J.H.; Rick, J.; Hwang, B.-J. Solid-state polymer nanocomposite electrolyte of $\text{TiO}_2/\text{PEO}/\text{NaClO}_4$ for sodium ion batteries. *J. Power Sources* **2015**, *278*, 375–381. [\[CrossRef\]](#)
70. Rao, C.V.S.; Ravi, M.; Raja, V.; Bhargav, P.B.; Sharma, A.K.; Rao, V.V.R.N. Preparation and characterization of PVP-based polymer electrolytes for solid-state battery applications. *Iran. Polym. J.* **2012**, *21*, 531–536.
71. Stephan, A.M.; Kumar, S.G.; Renganathan, N.G.; Kulandainathan, M.A. Characterization of poly (vinylidene fluoride–hexafluoropropylene)(PVdF–HFP) electrolytes complexed with different lithium salts. *Eur. Polym. J.* **2005**, *41*, 15–21. [\[CrossRef\]](#)
72. Zhang, Z.; Xu, K.; Rong, X.; Hu, Y.-S.; Li, H.; Huang, X.; Chen, L. $\text{Na}_3.4\text{Zr}_{1.8}\text{Mg}_0.2\text{Si}_2\text{PO}_{12}$ filled poly (ethylene oxide)/ $\text{Na}(\text{CF}_3\text{SO}_2)_2\text{N}$ as flexible composite polymer electrolyte for solid-state sodium batteries. *J. Power Sources* **2017**, *372*, 270–275. [\[CrossRef\]](#)
73. Lee, Y.-G.; Fujiki, S.; Jung, C.; Suzuki, N.; Yashiro, N.; Omoda, R.; Ko, D.-S.; Shiratsuchi, T.; Sugimoto, T.; Ryu, S.; et al. High-energy long-cycling all-solid-state lithium metal batteries enabled by silver–carbon composite anodes. *Nat. Energy* **2020**, *5*, 299–308. [\[CrossRef\]](#)
74. Louli, A.J.; Eldesoky, A.; Weber, R.; Genovese, M.; Coon, M.; deGooyer, J.; Deng, Z.; White, R.T.; Lee, J.; Rodgers, T.; et al. Diagnosing and correcting anode-free cell failure via electrolyte and morphological analysis. *Nat. Energy* **2020**, *5*, 693–702. [\[CrossRef\]](#)